Engineering Aspects–Computational Studies

Coupling Pediatric Ventricle Assist Devices to the Fontan Circulation: Simulations with a Lumped-Parameter Model

KEREM PEKKAN,* DAVID FRAKES,* DIANE DE ZELICOURT,* CAROL W. LUCAS,† W. JAMES PARKS,‡ AND AJIT P. YOGANATHAN*

In pediatric ventricular assist device (VAD) design, the process of matching device characteristics and dimensions to the relevant disease conditions poses a formidable challenge because the disease spectrum is more highly varied than for adult applications. One example arises with single-ventricle congenital defects, which demand palliative surgeries that create elevated systemic venous pressure and altered pulmonary hemodynamics. Substituting a mechanical pump as a right ventricle has long been proposed to eliminate the associated early and postoperative anomalies. A pulsatile lumped-parameter model of the single-ventricle circulation was developed to guide the preliminary design studies. Two special modules, the pump characteristics and the total cavopulmonary connection (TCPC) module, are introduced. The TCPC module incorporates the results of three-dimensional patient-specific computational fluid dynamics calculations, where the pressure drop in the TCPC anastomosis is calculated at the equal vascular lung resistance operating point for different cardiac outputs at a steady 60/40 inferior vena cava/superior vena cava flow split. Preliminary results obtained with the adult parameters are presented with no ventricle remodeling or combined larger-size single ventricle. A detailed literature review of single-ventricle function is provided. Coupling a continuous pump to the single-ventricle circulation brought both the pulmonary and systemic venous pressures back to manageable levels. Selected VADs provided an acceptable cardiac output trace of the single left ventricle, after initial transients. Remodeling of the systemic venous compliance plays a critical role in performance and is included in this study. Pulsatile operation mode with rotational speed regulation highlighted the importance of TCPC and pulmonary artery compliances. Four different pumps and three patient-specific anatomical TCPC pathologies were studied. Magnitudes of the equivalent TCPC resistances were found to be comparable to the vascular resistances of the normal baseline circulation, significantly affecting both the VAD design and hemodynamics. *ASAIO Journal* 2005; 51:618–628.

One important aspect in ventricular assist device (VAD) design is the process of matching the device characteristics and dimensions to the relevant disease conditions. Compared with the adult VAD applications,[1–3] this process poses a formidable challenge for pediatric applications because the disease spectrum is highly varied. In addition, unlike existing short-term VAD use like in bridge-to-transplant,[4] bridge-to-recovery,[5,6] rescue concepts, or long-term permanent replacement in stable adult circulation systems,[7,8] for pediatric applications[9] hemodynamic conditions are dynamic because they change drastically with growth, collateral angiogenesis, and corrective surgical interventions. These alterations influence the design specifications, design tools, and solution concepts of the VAD and place an emphasis on more flexibility and ease of control with respect to the changing conditions. A specific example is the range of congenital cardiac defects where there is cyanotic mixing between systemic and pulmonary circulation. This condition necessitates a series of complex surgical interventions that result in a single functioning ventricle.

Congenital cardiac defects that are amenable to a single-ventricle repair are the atrial septal defect, an atrioventricular canal defect, hypoplastic left heart syndrome, pulmonary atresia, D-transposition of the great arteries, ventricular septal defect, and tricuspid atresia. Surgical treatments[10] are palliative, performed in series, and result in complex three-dimensional morphologies and flow structures at the venous side (**Figure 1**). Unique circulation systems are created at each surgical repair with drastic physiologic and hemodynamic differences as compared with a normal circulation with a four-chambered heart (**Figure 2**). The final stage, the Fontan palliation or total cavopulmonary connection (TCPC), diverts all systemic venous blood to the pulmonary arteries with no parallel right ventricle to pump the blood through the pulmonary capillary bed. This single pumping action results in elevated systemic venous and caval pressure and altered pulmonary artery hemodynamics (reduced pulsatility, pulmonary arterial hypotension, and unequal hepatic blood distribution) with severe problems during the early and postoperative period.[11] Substituting a mechanical pump as a right ventricle that can "produce a step down in pressure energy of 5 mm Hg in

From the *Cardiovascular Fluid Mechanics Laboratory, Wallace H. Coulter Department of Biomedical Engineering, Georgia Institute of Technology, Atlanta, GA; †Biomedical Engineering Department, University of North Carolina, Chapel Hill, NC; and ‡Department of Pediatrics, Emory University School of Medicine, Sibley Heart Center Cardiology, Atlanta, GA.

Submitted for consideration April 2005, accepted in revised form May 2005.

Presented in part at the First International Conference on Pediatric Mechanical Circulatory Support Systems and Pediatric Cardiopulmonary Perfusion, May 19–22, Hershey, PA, USA.

Correspondence: Ajit P. Yoganathan, PhD, Wallace H. Coulter School of Biomedical Engineering, Georgia Institute of Technology & Emory University, Room 2119 U.A. Whitaker Building, 313 Ferst Dr., Atlanta, GA 30332-0535.

DOI: 10.1097/01.mat.0000176169.73987.0d

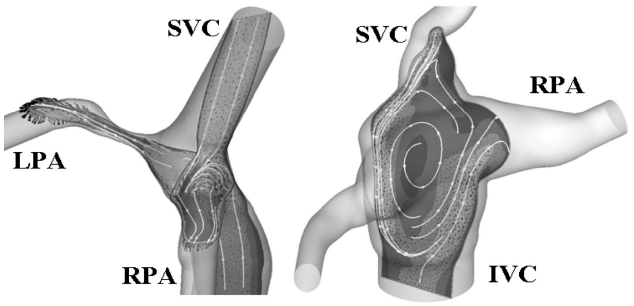

Figure 1. An extracardiac (**left**) and intraatrial (**right**) TCPC connection. The right heart is completely bypassed by the anastomosis of superior vena cava (SVC) and inferior vena cava (IVC) to the left (LPA) and right (RPA) pulmonary arteries. Snapshots of velocity magnitudes and streamlines in selected sections are obtained through computational fluid dynamics (CFD) demonstrating the complex flow fields that are encountered.

the inferior vena cava and producing a step up in pressure energy of 5 mm Hg in pulmonary arteries"[12] has long been proposed to eliminate these anomalies[13] and to reverse the "Fontan paradox" for improved quality of life.

Despite the growing practice and benefits of pediatric VAD use in numerous cardiac diseases,[14,15] there is still limited knowledge and experience of the VAD use for the cyanotic congenital heart defects. Current studies focus more on augmenting the postoperative management strategies with a pediatric VAD as an extension of the routine ECMO procedures[16] in the "rescue" groups. In contrast, the prophylactic use of VADs is described by Ungerleider *et al.*[17] for the early postoperative management of Norwood stage 1 patients. With the current management strategies, the overall survival of these patients is still very poor compared with the outcomes of the surgical stages that follow. Successful postoperative management of Norwood patients demands the maintenance of a delicate balance between the pulmonary and systemic vascular flows (Q_p/Q_s),[18] which can be accomplished more easily with a pediatric VAD.

Review of the earlier single-ventricle animal studies shows that "an acute TCPC model is very difficult to maintain and incompatible to the biventricular physiology. Unsupported acute bypass of the right heart causes volume shift into the high capacitance systemic venous circulation, reduced pulmonary blood flow, and low cardiac output. Meaningful hemodynamic stability beyond several hours was not achieved in these studies because of volume related complications."[13] These earlier findings are also confirmed by our ongoing experiments with lambs,[19] where eventual hemodynamic collapse follows the acute TCPC. Rodefeld *et al.*[13] recently demonstrated stable hemodynamics (with unchanged systemic venous and pulmonary artery pressures) in an acute TCPC model with a pair of axial VADs located at IVC and SVC. This suggests potential for

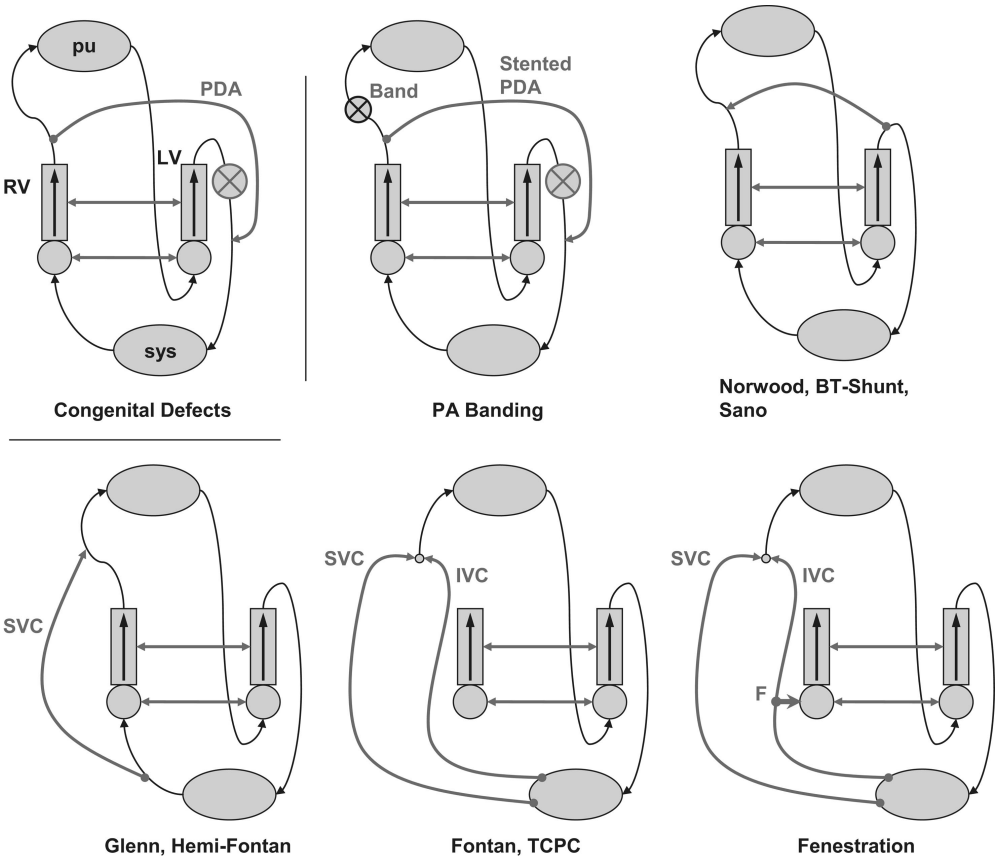

Figure 2. Circuit schematics of successive Fontan interventions. sys, systemic vascular bed; pu, pulmonary vascular bed; PDA, patent ductus arteriosus; RV, right ventricle; LV, left ventricle; SVC, superior vena cava; IVC, inferior vena cava; F, fenestration between the common atrium and the IVC. Arrows indicate the direction of blood flow and denotes any type of flow restriction.

augmenting pulmonary blood flow, during both early and late post-Fontan periods.

The hemodynamics of pulmonary support of a systemic univentricular chamber are still preliminary and further studies are warranted for quantitative understanding. Some of these aspects will be studied in this article. Hetzer et.al[15] reported no success in their congenital heart defect group (Group: Rescue) on pediatric biventricular or left ventricle support configurations (Berlin Heart VAD). For their other groups (bridge to transplant and acute myocarditis), the outcomes with the pediatric VADs were satisfactory. The development of effective treatment strategies for pediatric VADs necessitates greater emphasis on the congenital patient population.[20]

In this article, a reduced-order unsteady lumped-parameter mathematical model is used to offer further insight into this clinical problem. The main objective is to provide a flexible VAD design tool to aid the preliminary pump selection and design studies for future *in vitro* tests or computational models. Further down the road, this methodology, when combined with patient-specific catheterization data, could lead to quantitative treatment plans

Lumped-parameter models have been widely used in cardiovascular system applications.[21,22]. A subset of these incorporates VADs.[23,24] A recent review[25] provides further literature and summarizes different levels of sophistication. In congenital heart disease fluid dynamics, lump-parameter modeling is used integrated to the computational fluid dynamics (CFD) solution as a reduced-order cardiovascular system to provide the time-dependent inflow/outflow boundary conditions.[26,27] In a fully coupled lumped-parameter/CFD approach, the transient CFD solver and the relatively simple lumped-parameter solver proceed in time domain simultaneously during the course of numerical computations. Compared with a lumped-parameter model where hundreds of cardiac cycles can be traced in seconds using a standard PC, CFD solvers are computationally expensive because they tackle the nonlinear partial differential equations of fluid flow. For the three-dimensional anatomical TCPC models, even a small section of the cardiac cycle requires weeks of computational time in multiple high-performance computer clusters. For an integral solution approach as described above, the practical advantage of the simple lumped-parameter model is diminished because it should wait for the CFD solver to complete its computations. Therefore, the best use of lumped-parameter modeling involves prior conduction the computationally expensive CFD simulations to obtain the *characteristics* of the intended TCPC model. These are then introduced into the simple lumped calculations for fast extrapolative studies, where other system parameters are varied.

The current study is based on recent *in vitro* experimental and computational anatomical TCPC fluid flow results [28–30] where the actual patient-specific magnetic resonance imaging (MRI) and PC-MRI data are used. Flow and anatomy information is obtained for sedated patients with institutional review board-approved procedures and informed consent, representing the resting flow conditions. Combination of those patient-specific results with a lumped-parameter model facilitates a direct comparison of the local TCPC flow energetics to those of the entire normal or single-ventricle circulation. This study clearly highlighted one significant implication, the importance of hydrodynamic power loss at the TCPC junction for surgical improvements and VAD design. Clinical importance of this parameter has long been questioned in literature due to a lack of quantitative anatomical data and comparative studies.

Methods

Lumped-Parameter Model

A pulsatile lumped-parameter model of the single-ventricle circulation is developed to guide the preliminary design studies of an artificial pulmonary ventricle. A versatile mathematical model developed by Peskin *et al.* [31,32] is adopted here to explore different device options and operation scenarios. In this model, arteries and heart chambers are treated as pure and time-dependent compliance chambers with lumped capillary and valve resistances.[33] The circuit schematics are shown in **Figure 3**. One important advantage of this model is the ability to introduce additional chambers or shunts between any vascular compartments, an option that is useful modeling of congenital heart disease cases. The most common shunts, which are illustrated in **Figure 2**, are either surgically created or exist as a cardiac defect.

In this model the instantaneous flow rate from compartment *i* to compartment *j* is represented as:

$$Q_{ij} = (P_j\text{-}P_i) \cdot \frac{1}{R_{ij}} \cdot S_{ij} - \frac{L_{ij}\dot{Q}_{ij}}{R_{ij}} \cdot S_{ij} - Qp_{ij} \qquad (1)$$

The magnitude of the inertial frictional effects on the fluid per unit cross-sectional area can be estimated from $L_{ij} = 4\rho l/(\pi D)^2$ and is introduced in **Equation 1** as a lumped impedance for each compliant chamber. Vascular resistances, R_{ij} are available either from the cardiac catheterization data or from the literature. In this model, resistances through the heart valves are also modeled using the R_{ij} matrix. For heart valves, the impedance terms are kept zero to avoid further model complexities. S_{ij} can be either 0 or 1 based on the upstream and downstream pressures to control the valve states between the compartments. For a simple shunt, there is no valve between the compartments and $S_{ij} = 1$. For a general situation, $R_{ij} \neq R_{ji}$ and can be used to model a leaking valve. Qp_{ij} is the source term due to a ventricle assist pump, which will be discussed in the following section. Conservation of mass for each compliant node with a compliance of C_i leads to N ordinary differential equations:

$$\frac{d(C_iP_i)}{dt} = \sum_{j\text{-}1}^{N} j(Q_{ij} - Q_{ji} - Qp_{ij}) \qquad (2)$$

The unknown compartmental pressures, P_i for each chamber are then calculated at each time step by solving **Equation 2**. After an implicit Eulerian time discretization, source terms due to pumps and inertial effects lead to a set of nonlinear equations requiring iterative numerical techniques. The standard iterative Newton's method is used.[34]

To accomplish the objectives of this study, two additional modules are introduced to the basic model. These are the pump characteristics module and the TCPC module.

Pump Characteristics Module

The pump characteristics module includes the inertial effects and inlet and outlet cannula resistances as a function of flow rate.[23] A range of pump characteristics are studied with

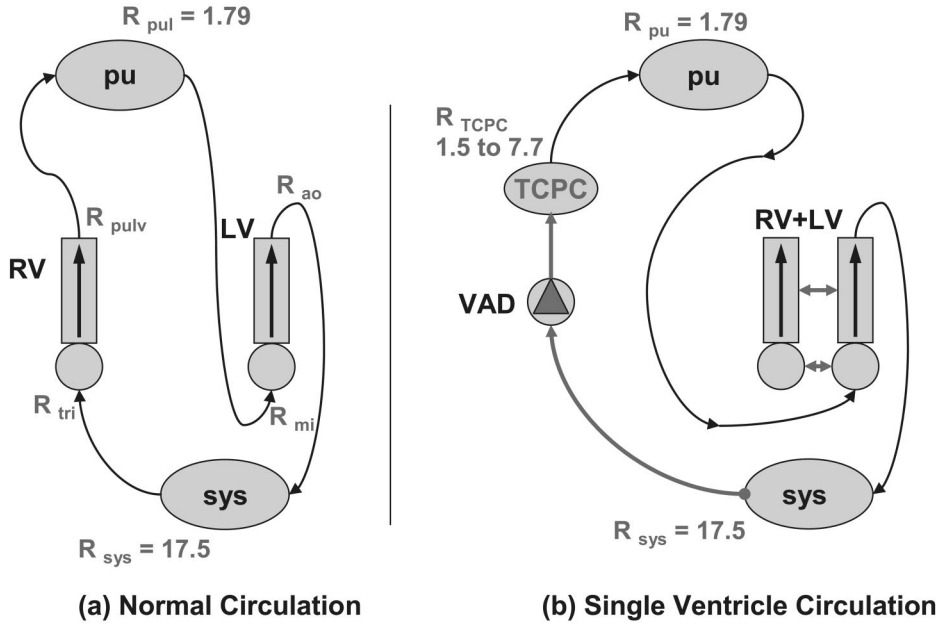

Figure 3. (**a**) Schematics of normal circulation—lumped representation of pulmonary and systemic beds. (**b**) Single-ventricle circulation with a pulmonary support pump (VAD)—after final-stage Fontan surgery. R_{TCPC} is the equivalent TCPC resistance calculated from *in vitro* experiments for the studied patient specific anatomies. R_{sys}, systemic vascular resistance; R_{pul}, pulmonary vascular resistance; RV, right ventricle; LV, left ventricle; pu, pulmonary bed (lungs); sys, systemic bed (upper and lower body combined). Arrows represent the blood flow directions and cardiac shunts. R_{tri}, tricuspid valve resistance; R_{pulv}, pulmonary valve resistance; R_{mi}, mitral valve resistance; R_{ao}, aortic valve resistance. All resistance values are in (mm Hg/l^{-1}·min^{-1}). For the single-ventricle circulation model (**b**), only mitral and aortic valves exist.

the given quadratic pressure-drop and flow rate relations shown in **Equation 3**:

$$Qp_{ij} = \sqrt{\frac{A \cdot w^2\text{-}(P_j\text{-}P_i)\text{-}Lptot_{ij} \cdot \dot{Q}p_{ij}}{Rptot_{ij}}} \qquad (3)$$

The terms of total resistance and inertance ($Rptot_{ij}$ and $Lptot_{ji}$) model the total internal pump resistance including the inlet/outlet cannulas. Qp_{ij} matrix is antisymetric where $Qp_{ij} = \neq -Qp_{ji}$. Cannula diameters are assumed same as the hydraulic vessel diameters of IVC and SVC. For the vessel sizes, average values from our anatomy database are used (12.7 mm and 19.5 mm for SVC and IVC, respectively, averaged over seven patients). Steady cannula resistances are then estimated using the laminar friction factor (*64/Re*).

A certain error is already introduced by specifying discrete lumped compliances/inertias and by neglecting the Womersley number effects in the velocity profile. For a complete and more accurate transient simulation, the actual unsteady pump characteristics should be used locally at pump inlets/outlets through the method of characteristics.[35] This level of sophistication was not tackled in the current study and was postponed for a future work. Therefore, the simulated pump operation is quasi-steady because the eight different actual unsteady operation zones of the pump are not considered. (This consideration becomes important only for the pulsatile simulations, because the venous side flow is steady for the single-ventricle circulation when respiration and other effects are neglected.) In the pulsatile pump simulations, pulsatility is introduced through a sinusoidal rotational speed (w) variation that is synchronous with the left heart.

TCPC Module

Computational Fluid Dynamics The TCPC module incorporates the results of three-dimensional patient-specific computational fluid dynamics (CFD) calculations where the pressure drop in the TCPC anastomosis is calculated at the equal vascular lung resistance operating point for different cardiac outputs at a steady 60/40 SVC/IVC flow split.[28,29] Calculation of the equal vascular lung resistance operating point is detailed in an earlier article.[30]

This approach generated the complete quasi-steady hydrodynamic characteristics of a given TCPC template at different cardiac outputs when the two lung resistances are equal. These characteristics can then be used in any lumped-parameter model with the desired level of sophistication. Characteristics of an intraatrial (TCPC1),[28] an extracardiac Fontan with severe LPA stenosis (TCPC2),[29] and a bilateral TCPC connection (TCPC3)[36] are studied.

The three-dimensional anatomical reconstructions for the CFD solutions were realized from the patient MRI data through an adaptive control grid interpolation technique.[37] The anatomical lumen surfaces were exported to GAMBIT (Fluent Inc., Lebanon, NH) for tetrahedral mesh generation. Mesh independency was achieved with around 500,000 and 450,000 four-node tetrahedral elements. Steady-state flow fields were then computed using the parallelized segregated finite-element CFD solver (FIDAP; Fluent Inc.). The pressure projection algorithm with the streamline upwinding scheme was used.[28] Fourth-order relative convergence for velocity and pressure was established starting with zero initial conditions for absolute change in solution vector via Euclidean norm, requiring approximately 6,000 computational iterations for the global

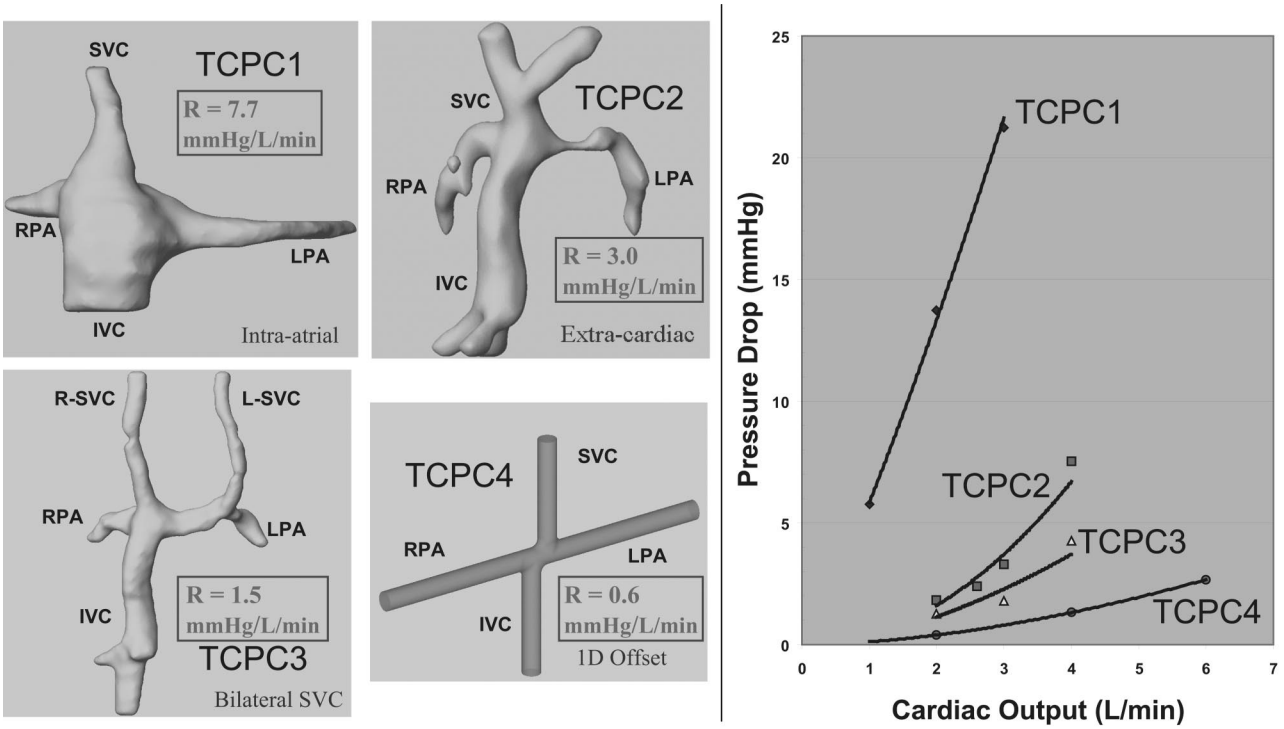

Figure 4. Selected TCPC anatomies and their calculated "equivalent resistance" values. The equivalent TCPC pressure drop (as calculated for combined IVC/SVC and LPA/RPA branches) versus total cardiac output is shown on the right graph for these TCPC models. Slope of a linear fit line corresponds to the reported "equivalent resistances," which are used in the lumped-parameter model. For comparison, for a normal circulation, systemic and pulmonary vascular resistances are ~17.5 and ~1.8 mm Hg·/$^{-1}$·min^{-1}.

convergence of all flow variables. All CFD jobs were run in parallel using a 28-node Linux computer cluster with 2.8 GHz processor speed and 2 GB memory per node.

Equivalent Resistance of the TCPC The lumped-parameter model requires the hydrodynamic flow resistance value at the TCPC junction. This can be calculated from the slope of the pressure drop versus cardiac output curve. However, defining a single pressure drop value that is representative of the TCPC is not straightforward because the actual TCPC pathway consists of two inlets and two outlets and creates complex fluid dynamic mixing at the junction. Averaging the pressures at outlets and inlets and subtracting them from each other may be an attractive approach and has been used in the earlier literature. However, this approach would overestimate the equivalent TCPC pressure drop because not all of the total cardiac output flows through the junction (*i.e.,* the total output is split). In this case, the basic resistance relation that is based on the Bernoulli equation cannot be valid because of the intense mixing within the junction. The correct approach involves the calculation of an "equivalent pressure drop" from the computational or measured hydrodynamic power loss values as given in **Equation 4**:

$$\Delta P_{equivalent} = \frac{\mathbb{P}_{loss}}{Q_{total}} \tag{4}$$

The hydrodynamic power that is consumed in the TCPC to overcome the flow resistance can be calculated through **Equation 5**:

$$\mathbb{P}_{loss} = \Sigma(P_{inlet} \cdot Q_{inlet}) - \Sigma(P_{outlet} - Q_{outlet}) \tag{5}$$

In **Equation 5**, average flow rate (Q) and stagnation pressure (P) values at the TCPC branches are obtained through *in vitro* experiments or computational simulations. The hydrodynamic power loss index represents both the pressure drop and global TCPC flow quality and has been established as a valid parameter for comparing the overall performance of different TCPC designs and surgical morphologies.[38]

For the studied TCPC anatomies, the calculated equivalent pressure drops (at the equal right/left vascular lung resistance operating point) versus the total cardiac output are plotted in **Figure 4**. For simplicity, a linear relation is assumed between flow and pressure and a regression line is fitted to the data. The slope of this line is defined as the "equivalent TCPC resistance" and used in our lumped-parameter model. The TCPC morphologies and the corresponding equivalent TCPC resistance values are presented in **Figure 4**. For some anatomies the linear equation fit has produced lower R^2 values, because for some models the actual pressure-flow relation of the TCPC is second or higher order (or more complex) where fluid resistances increase with increasing cardiac outputs. (R^2 values of the linear fit are 0.99, 0.92, 0.88, and 0.99 for TCPC 1, 2, 3, and 4, respectively.) For comparison, *in vitro* power loss results from our earlier reference one-diameter-offset model (TCPC4) are also included in **Figure 4**.[38]

Disease Conditions, Pediatric Lumped Parameters, and the Single-Ventricle Function It is a difficult task to characterize the complete hemodynamic evolution of congenital diseases during the course of treatments. For lumped-parameter analysis and VAD timing strategies, the complete course of events can be separated into 10 phases where the hemodynamic

Table 1. Literature Survey on Single-Ventricle Function and Hemodynamics Before and After Fontan Surgery

	Pre-Fontan	Post-Fontan
Systemic venous pressure (mm Hg)[43]	<10	10–18
Systemic venous compliance (ml/mm Hg)[45]	298 ± 15	1517 ± 678
Blood volume (ml/kg)[45]	70	79
Systemic vascular resistance[40]	20% below normal	75% increase after Fontan or Glenn
Effective Sys. arterial elastance (mm Hg/ml)[48]	2.1	2.4
Systolic blood pressure[49]	Normal	
Diastolic blood pressure[49]	Lower than normal	
Systolic function[43]		Suction effect on transpulmonary flow
Volume intercept of end-systolic PV relation, Vo (ml/m^2)[48]	9	11
End-systolic volume (ml/m^2)[50]	Increased compared to normal: 21–56	
End-systolic elastance (mm Hg/ml)[48]	5	3.1
Ventricular compliance[40]		Unchanged or enhanced, peak compliance shifted to the later portion of diastole (from the earlierportion)
Diastolic function		Should be good[43] Decreases[40] Well-maintained[53] Decrease gradually after Fontan[42]
End-diastolic volume	110% larger than the sum of left and right normal hearts[51] Increased compared with normal 77–137 ml/m^2 [50] 70 ml/m^2 200–300% normal (due to stage 1 volume overloading)[40]	100–120% normal[54] 77 ml/m^2 125–200% second stage (15% additional fall)[40]
Isovolume relaxation time		Prolongation, E/A ratio also reduced 95 ms at E_{wave} velocity = 40[53] Time constant of relaxation also increased by 37% (25.7 postoperatively to 18.7 ms)[40]
Pulmonary venous flow[52]	Occurs during diastole	Occurs during systole
Stroke volume	42 ml/m^2 [48] Increased compared to normal 58–80%[50]	37 ml/m^2 [48]
Ejection fraction	61%[48,49] Decreased from 72% to 58% compared with normal 0.55[51] 57% compared with normal 68%[55]	48%[48,49] Decreased to 39% 1 year after Fontan[55]
Heart rate[45,49,52]		Increased 9.5–17%
Aerobic capacity[56]		60% lower compared with age-matched normals

* Where appropriate, these parameters are used in the lumped-parameter model.

parameters stay more or less constant with distinct characteristics. These are: 1) fetal state, 2) neonate state until disease presentation, 3) course until the first intervention (usually NW I), 4) postoperative stage I, 5) before second-stage surgery, 6) postoperative bidirectional Glenn, 7) before Fontan stage, 8) postoperative Fontan, 9) fenestration issues, and 10) long-term course.

Application of a VAD is potentially possible during any of these stages, but the corresponding stage-specific hemodynamic parameters should be used in the planning. While there is still limited data available in the literature, patient-specific catheterization can be of assistance.

In this study, for the VAD timing, we considered the early postoperative phase after the corrective surgeries, either the Glenn or Fontan stage, where the volume loading of the left ventricle is reduced. Vascular and ventricle remodeling during the later course is essential but comprehensive. For example, the functional single left ventricle that is exposed to volume overload for longer periods demonstrated persistent abnormalities in ventricular function compared with cases with delayed second-stage or Fontan-stage surgeries.[39] For this preliminary study, an attempt is made only to represent the remodeling in the systemic venous system during the postoperative course. It is known that similar changes took place in the pulmonary vascular resistance and systemic vascular resistance.[40] Although limited data are available, there are cases where higher pulmonary vascular resistance values are dramatically lowered due to mechanical ventricular support.[41]

Pediatric lumped parameters and vascular function of the single ventricle are not common in the literature. Limited data are available, and relevant cases are summarized in **Table 1**. Adult parameters are used for the baseline healthy circulation

and for other unavailable data. Because a complete characterization was not available for left ventricle remodeling or cardiac output increase due to a single ventricle, these effects are not simulated here and were postponed for future studies.

Results

TCPC State (Single-Ventricle Circulation)

The early postoperative or acute TCPC state with a single operating ventricle is simulated by removing the right ventricle (with the tricuspid and pulmonary valves) and having systemic, pulmonary, and TCPC resistances in series. In this model, among other lumped variables, systemic venous compliance is found to be critical in achieving the elevated systemic pressures (10–18 mm Hg) of the Fontan physiology. Indeed, for this simple single-ventricle configuration, reasonable cardiac outputs can only be achieved with such an elevated pressure state.

A first set of simulations was conducted using the baseline compliance (1.75 l/mm Hg) in combination with the baseline (pre-Fontan) venous pressure (2 mm Hg) values. This resulted in: Very low cardiac outputs (0.20 l/min for TCPC1 and 0.46 l/min for TCPC3). Low systemic pressure that would not increase to the elevated levels observed during the post-Fontan period (only <1 mm Hg could be obtained). This was due to the high baseline systemic venous compliance. Specifying a high venous pressure value (10 mm Hg) as an initial condition did improve the cardiac outputs (1.00 l/min for TCPC1 and 2.40 l/min for TCPC3), but only slightly increased the final venous pressure (1 mm Hg).) Subnormal arterial pressure variation (30/25 mm Hg for TCPC1 and 60/44 mm Hg for TCPC3). A large blood volume to back-up this high systemic venous pressure (10 mm Hg × 1.75 l/mm Hg = 18 l).

This last result correlates well with the clinical observations of peripheral edema, systemic fluid deposition, abdominal swelling, and fatigue that are common in the postoperative Fontan patient.[42] For the single-ventricle circulation, gravity significantly opposes the venous return while inspiration exerts a marked increase in hepatic venous flow.[43] Likewise, postoperative treatments routinely involve the utilization of gravity to aid venous return to the heart (patient head and legs are positioned upwards) and mechanical ventilation.[44] These suggest that remodeling of the venous compliance (a decrease) may take place during the early postoperative period. During this period, blood volume shift to the systemic venous vasculature can temporarily maintain the cardiac output as indicated in our simulations. Likewise, compliance measurements for post-Fontan patients showed a drastic reduction (400%) from normal values (**Table 1**).[45] A good review of venous physiology is available in literature.[46]

In the following simulations, we use the post-Fontan conditions tabulated in **Table 1** when appropriate and modeled the compliance regulation. Postoperative systemic compliance regulation is made possible by an inverse exponential compliance dependence to pressure. Post-Fontan venous compliance that is given in **Table 1** is attained in a specified course of time starting with the baseline value (pre-Fontan). This remodeling duration is specified as a relaxation factor in the systemic venous compliance pressure dependence curve. **Figure 5** shows the venous systemic pressure histories for the two TCPC models. These simulations resulted in: Reasonable cardiac outputs (1.50 l/min for TCPC1 and 3.34 l/min for TCPC3) Systemic pressure that gradually rose to approximately 15 mm Hg. Realistic systemic blood volume reserves. Decreasing pulmonary artery pressure with increasing equivalent TCPC resistance (4.2 mm Hg for TCPC1 and 9.4 mm Hg for TCPC3). Arterial pressures of 46/37 mm Hg and 80/63 mm Hg for TCPC1 and TCPC3, respectively, at periodic steady state (**Figure 5**). Nearly nonexistent pulsatility in the venous return (magnitude of the pressure variations < 0.1 mm Hg).

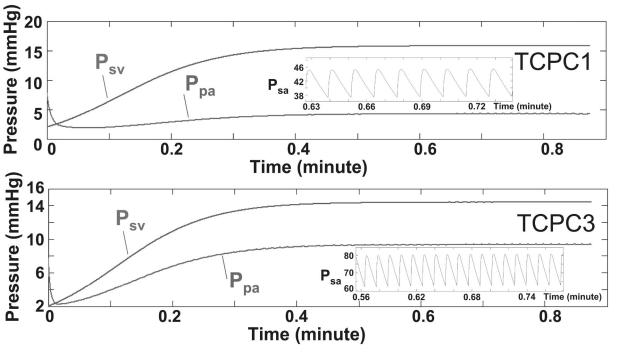

Figure 5. Systemic venous pressure increase after acute TCPC for two different TCPC models. This figure simulates the process of post-Fontan systemic venous compliance remodeling. Inserts show the arterial pressure pulse (in mm Hg). P_{sv}, systemic venous pressure; P_{pa}, pulmonary arterial pressure; P_{sa}, systemic arterial pressure.

This TCPC state is selected as the baseline disease condition for further comparative studies with venous assist devices and configurations.

Operating Points for Different Right VAD Characteristics

One possible assist pump configuration is to use two separate pumps located at IVC and SVC (**Figure 6**).[13] Four different pump characteristics are coupled to this configuration with different ranges of pressure heads and flow rates (**Figure 7**). Other configurations that could be more advantageous are also possible. They can be analyzed using the same techniques and are further detailed in the Discussion.

Reversal of the Fontan Paradox (VAD-Assisted Single-Ventricle Circulation)

As expected,[12] introducing a right VAD to the single-ventricle circuit decreased the systemic venous pressure and increased the pulmonary arterial pressure to manageable levels. Remodeling of the "lower" post-Fontan systemic venous compliance to normal (higher) levels is again crucial and included in our model as described earlier. This process is simulated in **Figure 8** for TCPC3 using PUMP-1 and for TCPC1 using PUMP-4, where the systemic venous pressures were gradually lowered due to the action of a VAD.

Continuous-Flow Pumps

In **Figure 7**, the operating points that are reached after including a right ventricle assist continuous pump to the circuit with TCPC1 and TCPC3 models are indicated and tabulated in **Table 2**. It must be emphasized that these points correspond to

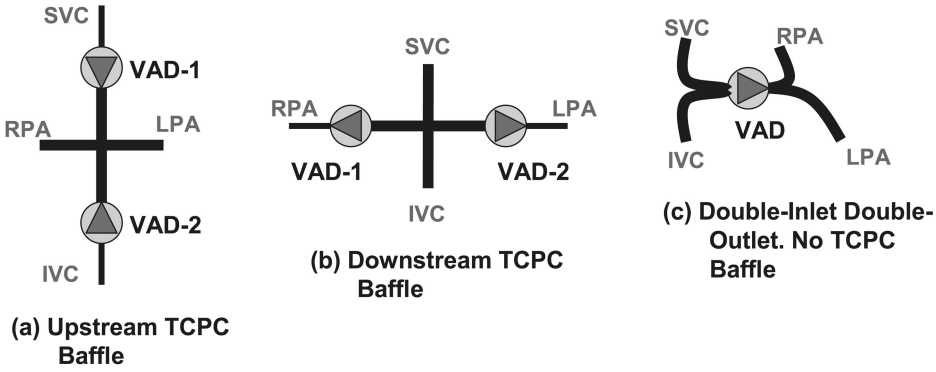

Figure 6. Possible ventricle assist device (VAD) configurations for pulmonary support.

the *mean* operating points with the average values of pressures and flow rates. An actual time history of various parameters is presented in **Figure 8** for the TCPC3-PUMP1 combination.

For each TCPC model, the required pump characteristic that induces approximately 5 l/min cardiac output and 15mm Hg elevation in pulmonary artery pressure is also calculated. These are indicated as the "design" pump characteristics in **Table 2**, which summarizes the flow properties of all the operation points that have been studied.

Higher pressures are observed in the region between the pump outlet and the TCPC baffle (indicated as P_{TCPC} in Table 2), where the actual TCPC resistance is located. Reducing the compliance at this region eliminated the problem but with a significant decrease in the pulmonary artery pressure. These values emphasize the influence of upstream compliance in canula design.

Pulsatile-Flow Pumps

To illustrate a pulsatile operation condition at the right side, the pump rotational speed is modulated sinusoidally (±200 rpm) during the course of operation for PUMP1 with TCPC3. These results are plotted in **Figure 9**. Pulsatility in the pulmonary system caused an apparent decrease in the impedance, leading to higher arterial pressures and cardiac outputs. The pump rotational speed was chosen to be synchronous with the left heart.

Pulsatility with rotational speed modulation is found to be limited due to relatively high pulmonary artery and TCPC baffle compliances. Although ±200 rpm variation was expected to produce approximately ±4.5 mm Hg of pulsatility, this has not been observed due to chamber compliances. Higher pulsatility indices are observed (±3.5 mm Hg) in the stiff TCPC baffle than in the upstream pulmonary artery (±1.5 mm Hg). The compliance used for the TCPC baffle was 10 times lower than the pulmonary artery compliance. Pulmonary artery flow and pressure pulsatility for a normal adult circula-

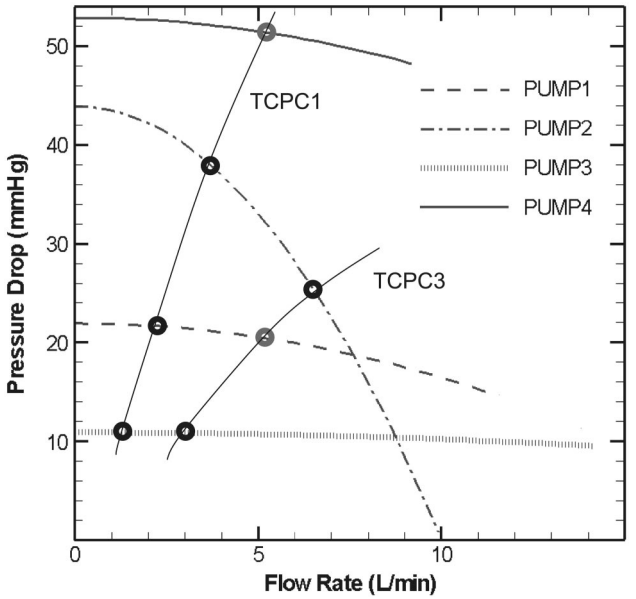

Figure 7. Pump characteristics and "with VAD" operating points (marked as circles) for TCPC1 and TCPC3.

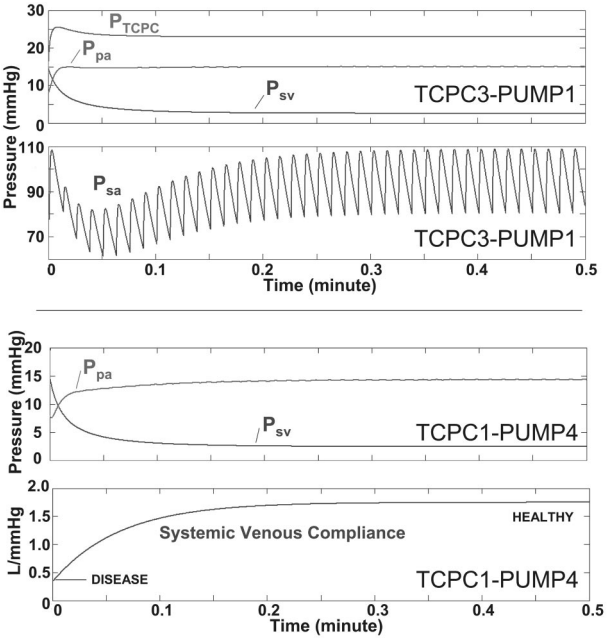

Figure 8. Reversal of the Fontan paradox. Recovery to the normal systemic venous pressures via VAD for TCPC3 (**top**) and TCPC1 (**bottom**). For TCPC1-PUMP4 configuration, systemic venous compliance remodeling change from diseased to healthy conditions is illustrated (**bottom**). P_{TCPC} represents the TCPC pathway pressure, which is located between the VAD outlet canula and TCPC junction.

Table 2. Operating Points of TCPC1 and TCPC3 for Selected VAD Characteristics

	P_{PA} (mm Hg)	P_{SV} (mm Hg)	Q_T (l/min)	P_{SA} (mm Hg)	P_{TCPC} (mm Hg)
TCPC1					
Pump 1	6.3	1.94	2.3	47/34	24
Pump 2	10.5	1.8	3.8	76/56	40
Pump 3	3.5	2.1	1.2	27/20	13
Pump 4*	14.0	1.7	5.1	102/75	53
TCPC3					
Pump 1*	14.5	1.77	5.2	105/77	22
Pump 2	17.9	1.63	6.4	128/95	27
Pump 3	8.4	1.95	3.0	62/46	13
Normal	22/10	2.3	5.1	117/89	—

Asterisk indicates the "design" condition with hemodynamic parameters closed to physiological levels indicated as "normal." P_{PA}, pulmonary artery pressure; P_{SV}, systemic venous pressure; Q_T, total cardiac output; P_{SA}, systemic artery pressure; P_{TCPC}, TCPC baffle pressure.

tion is provided in **Figure 9** as a reference and as a "gold standard."

Discussion

VAD Operation and Timing Single-ventricle pathologies are encountered in 2 per 1,000 live births, and clinicians report that a disproportionate (50%) amount of their time is occupied for the care of single-ventricle patients. Ventricle assist devices with further improvements and flexible strategies can simplify pre- and postsurgery management. Once the complete remodeling physiology that leads to the stable single-ventricle hemodynamics is known, VAD devices can help the patients to bridge this process with fewer complications. Long-term use of these devices for pediatric application may also be possible with faultless mechanical design and ultralow blood damage.

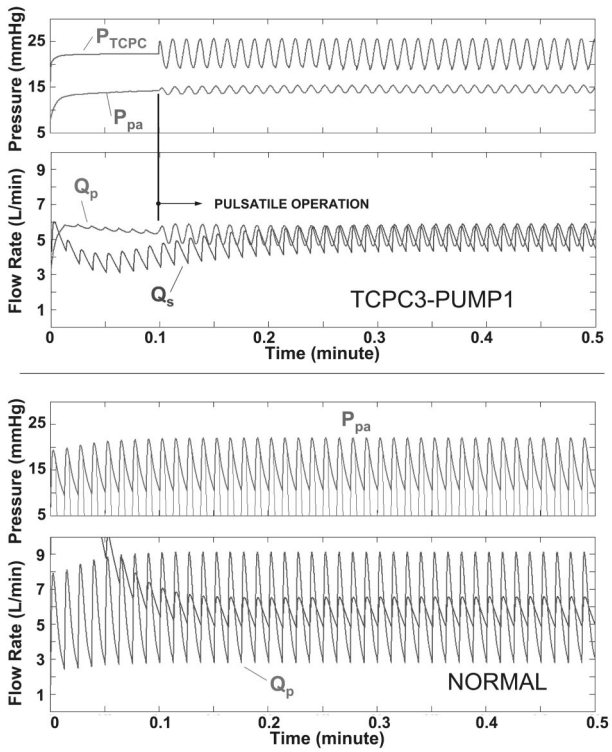

Figure 9. Top two figures: Continuous versus pulsatile operation. Pulsatility is induced by rotational speed modulation (±200 rpm). Modulation starts at t = 0.1 minutes. Pulmonary artery (P_{pa}) and TCPC baffle pressures (P_{TCPC}) are also shown. Pulsatility is further damped out in the pulmonary artery due to increased compliance. Corresponding pulmonary (Q_p) and systemic (Q_s) flow rate traces. **Bottom two figures:** Corresponding pulsatility for the normal circulation with a healthy right ventricle.

In this study, although one type of pump configuration (where the TCPC is located upstream to the VAD, **Figure 6a**) is studied, two other configurations are also possible. One configuration (**Figure 6b**) similarly uses two separate pumps, but they are now located upstream at LPA and RPA instead of IVC and SVC. The other configuration is to use a double inlet and outlet configuration in place of the TCPC (**Figure 6c**). The advantage of using two pumps is the ease of modulation of the SVC and IVC flow rates depending on the changing flow requirements (IVC/SVC flow split is more or less equal [50/50] in infants, but IVC flow increases as the child grows and reaches 60/40) and different downstream properties (like upper and lower body impedance and compliances). For this configuration, TCPC flow dynamics (resistance and compliance) becomes important and together with the left and right vascular lung resistances determines the LPA/RPA split. The equivalent TCPC resistance, which is located at the upstream of the assist pumps, seems to be an important factor. Moreover, the surgical Gore-Tex graft with a lower compliance may be present between the IVC pump outlet and the pulmonary arteries, which can cause higher local pressures at this region. A variation of this two-pump configuration is obtained when the pumps are located at the LPA and RPA branches (**Figure 6b**). This configuration may be undesirable because of cavitation problems and complications with graft collapse or buckling.

The double-inlet double-outlet configuration (**Figure 6c**) that avoids the TCPC resistance can be further preferred for its simplicity and ease of operation. It should be noted that for this configuration, there exits an internal pump resistance and additional inflow/outflow canula resistances, but these are lower in magnitude, internal to the pump, and do not complicate graft/vessel mismatch considerations.

During the reversal of Fontan paradox, flow rates should be chosen with considerations on the systemic venous capacitance because there is the possibility of collapsing the systemic venous return with very high uncontrolled flow rates. This can occur for the family of pump characteristics used in this article, especially during the early start-up, for a high-flow rate/low-head pump with lower the upstream TCPC compliance. Actual physiology of this condition[46] is complex to model mathematically because additional venous resistances are introduced by the body as a regulatory mechanism to avoid the drainage of the whole systemic venous blood.

Compared with continuous pumps, the use of pulsatile pumps is advantageous without debate. A simple rotational modulation scheme of the continuous pump, as used here, did not provide the physiologic pulmonary artery pulsatility. Rotational speed modulation may be suitable for left heart use where the compliances are significantly higher compared with the right side. Therefore, positive displacement pumps may be preferred for right heart support. Moreover, other synchroni-

zation schemes may be worth exploring in future studies. In our pulsatile configuration we used no valves. Configurations that use valves (a VAD with a nonreturn valve), despite the increase in blood damage, can increase the pulmonary artery pulsatility.

Replacing an existing TCPC with a VAD can generate drastic changes in the circulation because the hemodynamic and the heart has already modeled. Therefore, for long-term TCPC patients the inclusion of a pump, when required, can be considered in stages similar to those used for corrective surgeries.

Lumped-Parameter Model. Although a lumped-parameter mathematical model is practical and provides unsteady hemodynamics with fewer computational resources, its limitations have been highlighted in the literature extensively. For our model, future studies will involve the use of actual patient catheterization data for the unknown parameters where adult values are now substituted. For higher levels of pulsatile operation at the venous side, exact unsteady pump characteristics should be used. Moreover, other regulation and control modes need to be considered.

In our lumped TCPC characteristics module, we did not include the inertial effects of the TCPC pathway because all our *in vitro* and computational studies characterized the TCPC for the steady operation mode. Calculation of the transient characteristics (unsteady response) of the TCPC pathway is underway and will be presented in a future communication. Moreover, the *in vivo* unsteady fluid dynamics is extremely complex and involves effects of respiration and heart motion. Likewise, transient operation modes of the heart valves were not included in this simple model.

Clinical Observations and Significance. It is remarkable to note that the simple lumped-parameter model simulated the acute TCPC state, compatible with the observed hemodynamics of acute animal experiments. The importance of systemic venous compliance and flow resistances of the venous pathway is demonstrated and quantified. The remodeling of venous compliance may be important compared with venous resistance and deserves further clinical appreciation. The mean pulmonary artery pressure is 15 mm Hg before bidirectional Glenn surgery, 9.9 mm Hg before TCPC, 10.9 mm Hg after TCPC, and 8.5mm Hg 1 year after TCPC.[47] These data suggest a decrease in pulmonary artery pressures at the long-term post-Fontan, which is comparable to what we found in our computations. Unchanged pulmonary artery pressure just after the repair operations may be due to postoperative treatments and pulmonary remodeling physiology. Furthermore, our calculations do not included the common AV valve complications causing elevated pulmonary venous pressures, elevated pulmonary arterial pressures, and systemic venous pressures as a cascade.[42]

Conclusion

This study demonstrated the possibility and quantified the operation of a right ventricle assist device for full pulmonary support when there is no right ventricle. For two different patient specific TCPC anatomies, preliminary designs of two right VADs leading approximately 5 l/min total cardiac output and physiologic mean pulmonary artery and systemic venous pressures are presented. Starting with an acute poor postoperative state, arterial pressures and cardiac outputs are gradually brought to acceptable levels. The elevated systemic venous Fontan pressures decrease by the simultaneous action of the VAD and the remodeling process of the systemic venous compliance. Pulsatile operation mode at the venous side is quantified where the pulmonary artery pulsatility dependents on the upstream compliance. Rotational speed modulation did not provide the required physiologic pulmonary artery pulsatility.

Various configurations, strategies, and timing are possible for VAD use in a congenital patient population. Only a particular disease state is considered here, which demonstrated the importance of the systemic venous compliance besides other hemodynamic parameters. For the first time, an acute TCPC state is modeled using the lumped-parameter model, where lower equivalent TCPC resistances lead to significantly higher cardiac outputs. Moreover, for circulations with lower TCPC resistances, low-performance VADs are needed to maintain physiologic levels. These findings demonstrate the clinical importance of TCPC fluid dynamics both with and without ventricle assist. Equivalent TCPC resistances for anatomical models are in the same order of magnitude as the vascular resistances of the body. Lower TCPC resistances should imply better quality of life and exercise tolerance.

The presented lumped-parameter VAD model simplifies a complex clinical problem that requires further *in vitro* validation studies and animal experiments. The presented methodology is versatile enough to provide preliminary data for other interventional stages, such as those involving shunts, and can provide boundary conditions for detailed studies.

References

1. Wheeldon DR: Mechanical circulatory support: state of the art and future perspectives. *Perfusion* 18: 233–243, 2003.
2. Norman JC: The role of assist devices in managing low cardiac output. *Cardio Dis Texas Heart Inst Bull* 8: 119–152, 1981.
3. Yamane T: The present and future state of artificial heart technology. *J Artif Organs* 5: 149–155, 2002.
4. Hetzer R, Henning E, Schiessler A, *et al*: Mechanical circulatory support and heart transplantation. *J Heart Lung Transplant* 11: 175–181, 1992.
5. Müller J, Wallukat G, Weng Y: Weaning from mechanical cardiac support in patients with idiopathic dilated cardiomyopathy. *Circulation* 96: 542–549, 1997.
6. Kumpati GS, McCarthy PM, Hoercher KJ: Left ventricle assist device as a bridge to recovery: present status. *J Card Surg* 16: 294–301, 2001.
7. Frazier OH: Evolution of Battery-Powered, Vented Left Ventricular Assist Devices. *Ann Thorac Surg* 61: 393–395, 1996.
8. Mielniczuk L, Mussivand T, Davies R: Patient selection for left ventricular assist devices. *Artif Organs* 28: 152–157, 2004.
9. Sidiropoulos A, Hotz H, Konertz W: Pediatric circulatory support. *J Heart Lung Transplant* 11: 1172–1176, 1998.
10. Bove EL, Mosca RS: Surgical repair of the hypoplastic left heart syndrome. *Prog Pediatr Cardiol* 5: 23–35, 1996.
11. Cochrane AD, Brizard CP, Penny DJ: Management of the univentricular connection: are we improving? *Eur J Cardiothorac Surg* 12: 107–115, 1997.
12. de Leval MR: The Fontan circulation: What we have learned? What to expect? *Pediatr Cardiol* 19: 316–320, 1998.
13. Rodefeld M, Boyd CH, Myers CD: Cavopulmonary assist: circulatory support for the univentricle Fontan circulation. *Ann Thorac Surg* 76: 1911–1916, 2003.
14. Hotz H, Linneweber J, Dohmen PM: Bridge-to-recovery from acute myocarditis in a 12-year-old child. *Artif Organs* 28: 587–599, 2004.
15. Hetzer R, Loebe M, Potapov EV: Circulatory support with pneu-

matic paracorporeal ventricular assist device in infants and children. *Ann Thorac Surg* 66: 1498–1506, 1998.
16. Pizarro C, Davis DA, Healy RM, *et al*: Is there a role for extracorporeal life support after stage I Norwood? *Eur J Cardiothorac Surg* 19: 294–301, 2001.
17. Ungerleider RM, Shen I, Yeh T: Routine mechanical ventricular assist following the Norwood procedure – Improved neurologic outcome and excellent hospital survival. *Ann Thorac Surg* 77: 18–22, 2004.
18. Charpie JR, Kulik TJ: Pre- and post-operative management of infants with hypoplastic left heart syndrome. *Prog Pediatr Cardiol* 5: 49–56, 1996.
19. Ketner ME, Lucas CE, Mill MR, *et al*: Energy, hemodynamics, and respiration effects in lambs with various Fontan circulations. Paper presented at the BMES Annual Fall Meeting, Philadelphia, PA, October 2004.
20. Undar A, McKenzie ED, McGarry MC: Outcomes of congenital heart surgery patients after extracorporeal life support at Texas Children's Hospital. *Artif Organs* 28: 963–966, 2004.
21. Pennati G, Fiore GB, Lagana K, Fumero R: Mathematical modeling of fluid dynamics in pulsatile cardiopulmonary bypass. *Artif Organs* 28: 196–209, 2004.
22. Geven MCF, Bohte VN, Aarnoudse WH: A physiologically representative in vitro model of the coronary circulation. *Physiol Meas* 25: 891–904, 2004.
23. Vandenberghe S, Segers P, Meyns B, Verdonck P: Unloading effect of a rotary blood pump assessed by mathematical modeling. *Artif Organs* 27: 1094–1101, 2003.
24. Giridharan GA, Ewert DL, Pantalos GM: Left ventricular and myocardial perfusion responses to volume unloading and afterload reduction in a computer simulation. *ASAIO J* 50: 512–518, 2004.
25. Smith BW, Chase GJ, Nokes RI, *et al*: Velocity profile method for time varying resistance in minimally cardiovascular models. *Phys Med Biol* 48: 3375–3387, 2003.
26. Dubini G, de Laval, MR, Pietrabissa R, *et al*: A numerical fluid mechanical study of repaired congenital heart defects. Application to the total cavopulmonary connection. *J Biomech* 29: 111–121, 1996.
27. Lagana K, Balossino R, Migliavacca F: Multiscale modeling of the cardiovascular system: application to the study of pulmonary and coronary perfusions in the univentricular circulation. *J Biomech* 38: 1129–1141, 2005.
28. Pekkan K, Zelicourt D, Ge L: Flow physics driven CFD modeling of complex anatomical flows: A TCPC case study. *Ann Biomed Eng* 33: 284–300, 2005.
29. Pekkan K, Kitajima H, Forbess J: *Total cavopulmonary connection flow with functional left pulmonary artery stenosis: Fenestration and angioplasty in vitro. Circulation,* in press.
30. de Zelicourt DA, Pekkan K, Wills L, *et al*: In vitro flow analysis of a patient specific intra-atrial TCPC. *Ann Thorac Surg* 79: 2094–2102, 2005.
31. Peskin CS, Tu C: Hemodynamics in congenital heart disease. *Comput Biol Med* 16: 331–59, 1986.
32. Tu C, Peskin CS: Hemodynamics in transposition of the great arteries with comparison to ventricular septal defect. *Comput Biol Med* 19: 95–128, 1989.
33. Suga H, Sagawa K: Instantaneous pressure-volume relationships and their ratio in the excised, supported canine left ventricle. *Circ Res* 35: 117–26, 1974.
34. Kelley CT: *Solving Nonlinear Equations with Newton's Method.* Philadelphia, SIAM Press, 2003.
35. Fox JA: *Transient Flow in Pipes: Open Channels and Sewers.* West Sussex, Ellis Horwood, 1989.
36. Zelicourt D: A fluid mechanical assessment of anatomical models of the total cavopulmonary connection (TCPC) [MSc thesis]. Atlanta, Georgia Institute of Technology, 2005.
37. Frakes D, Conrad C, Healy T: Application of an adaptive control grid interpolation technique to morphological vascular reconstruction. *IEEE Trans Biomed Eng* 50: 197–206, 2003.
38. Ensley A, Lynch P, Lucas C: Toward designing the optimal total cavopulmonary connection: An in vitro study. *Ann Thorac Surg* 68:1384–1390, 1999.
39. Milanesi O, Stellin G, Colan SD: Systolic and diastolic performance late after Fontan procedure for a single ventricle and comparison of those undergoing operation at <12 months of age and at >12months of age. *Am J Cardiol* 89: 276–280, 2002.
40. Colan S: Systolic and diastolic function of the univentricular heart. *Prog Pediatr Cardiol* 16: 79–87, 2002.
41. Petrofski JA, Hoopes CW, Bashore TM: Mechanical ventricular support lowers pulmonary vascular resistance in a patient with congenital heart disease. *Ann Thorac Surg* 75: 1005–1007, 2003.
42. Gersony DR, Gersony WM: Management of the postoperative Fontan patient. *Prog Pediatr Cardiol* 17: 73–79, 2003.
43. Rychik J, Cohen MI: Long-term outcome and complications of patients with single ventricle. *Prog Pediatr Cardiol* 16: 89–103, 2002.
44. Fiorito B, Checchia PA: A review of mechanical ventilation strategies in children following the Fontan procedure. *Imag Paediatr Cardiol* 11: 4–11, 2002.
45. Kelley JR, Mack GW, Fahey JT: Diminished venous vascular capacitance in patients with univentricle hearts after the Fontan operation. *Am J Cardiol* 76: 158–163, 1995.
46. Goldberg HS, Rabson J: Control of cardiac output by systemic vessels. *Am J Cardiol* 47: 696–702, 1981.
47. Tanoue Y, Kado H, Shiokawa Y, *et al*: Midterm ventricular performance after Norwood procedure with right ventricular-pulmonary artery conduit. *Ann Thorac Surg* 78: 1965–1971, 2004.
48. Nogaki M, Senzaki H, Masutani S: Ventricular energetics in Fontan circulation: Evaluation with a theoretical model. *Pediatr Int* 42: 651–657, 2000.
49. Driscoll DJ: Exercise responses in functional single ventricle before and after Fontan operation. *Prog Pediatr Cardiol* 2: 44–49, 1993.
50. Sandor GGS, Patterson MWH, LeBlanc, JG: Systolic and diastolic function in tricuspid valve atresia before the Fontan operation. *Am J Cardiol* 73: 292–297, 1994.
51. Shimazaki Y, Kawashima Y, Mori T: Ventricular volume characteristics of single ventricle before corrective surgery. *Am J Cardiol* 45: 806–810, 1980.
52. Fogel MA, Donofrio MT: Comparison of patterns of pulmonary venous blood flow in the functional single ventricle heart after operative aorto-pulmonary shunt versus superior cavo-pulmonary shunt. *Am J Cardiol* 80: 922–926, 1997.
53. Penny DJ, Redington AN: Diastolic ventricular function after the Fontan operation. *Am J Cardiol* 69: 974–975, 1992.
54. Nakae S, Imai Y, Harada Y: Assessment of left ventricular function before and after Fontan's operation for the correction of tricuspid atresia. Changes in the left ventricular function determined by the left ventricular volume change. *Heart Vessels* 1: 83–88, 1985.
55. Parikh SR, Hurwitz RA: Ventricular function in the single ventricle before and after Fontan surgery. *Am J Cardiol* 67: 1390–1395, 1991.
56. O'Leary PW: Prevalence, clinical presentation and natural history of patients with single ventricle. *Prog Pediatr Cardiol* 16: 31–38, 2002.